Title

Effects of Veliparib on Microglial Activation and Functional Outcomes after Traumatic Brain Injury in the Rat and Pig.

Journal

Journal of neurotrauma, 35(7)

ISSN

0897-7151

Authors

Irvine, Karen-Amanda
Bishop, Robin K
Won, Seok Joon
et al.

Publication Date

2018-04-01

DOI

10.1089/neu.2017.5044

Peer reviewed

JOURNAL OF NEUROTRAUMA 35:918–929 (April 1, 2018)

DOI: 10.1089/neu.2017.5044

Effects of Veliparib on Microglial Activation and Functional Outcomes after Traumatic Brain Injury in the Rat and Pig

Karen-Amanda Irvine,[1] Robin K. Bishop,[1] Seok Joon Won,[1] Jianguo Xu,[1,2] Katherine A. Hamel,[3] Valerie Coppes,[3] Pardeep Singh,[1] Andrew Sondag,[1] Eric Rome,[1] Jayinee Basu,[1] Giordano Fabricio Cittolin-Santos,[1,4] S. Scott Panter,[3] and Raymond A. Swanson[1]

Abstract

The inflammation response induced by brain trauma can impair recovery. This response requires several hours to develop fully and thus provides a clinically relevant therapeutic window of opportunity. Poly(ADP-ribose) polymerase inhibitors suppress inflammatory responses, including brain microglial activation. We evaluated delayed treatment with veliparib, a poly(ADP-ribose) polymerase inhibitor, currently in clinical trials as a cancer therapeutic, in rats and pigs subjected to controlled cortical impact (CCI). In rats, CCI induced a robust inflammatory response at the lesion margins, scattered cell death in the dentate gyrus, and a delayed, progressive loss of corpus callosum axons. Pre-determined measures of cognitive and motor function showed evidence of attentional deficits that resolved after three weeks and motor deficits that recovered only partially over eight weeks. Veliparib was administered beginning 2 or 24 h after CCI and continued for up to 12 days. Veliparib suppressed CCI-induced microglial activation at doses of 3 mg/kg or higher and reduced reactive astrocytosis and cell death in the dentate gyrus, but had no significant effect on delayed axonal loss or functional recovery. In pigs, CCI similarly induced a perilesional microglial activation that was attenuated by veliparib. CCI in the pig did not, however, induce detectable persisting cognitive or motor impairment. Our results showed veliparib suppression of CCI-induced microglial activation with a delay-to-treatment interval of at least 24 h in both rats and pigs, but with no associated functional improvement. The lack of improvement in long-term recovery underscores the complexities in translating anti-inflammatory effects to clinically relevant outcomes.

Keywords: axonal injury; IL1-ß; MMP9; TNFα

Introduction

The mechanical tissue injury caused by brain trauma induces a local inflammatory response consisting of an initial microglial activation followed by infiltration of blood-born leukocytes and reactive astrocytosis. This innate immune response likely evolved as a first line of defense against the microbial infections that commonly accompany tissue injury and may also play a role in wound healing[1]; however, it can also have cytotoxic effects and suppress the neurite outgrowth and neurogenesis thought to underlie long-term functional recovery.[2–6] Given that the post-injury inflammatory response takes several hours to develop fully, anti-inflammatory intervention has been identified as a promising therapeutic approach to improving outcome from traumatic brain injury.[7]

Drugs that inhibit poly(adenosine diphosphate [ADP])-ribose polymerases (PARPs) have potent systemic and central nervous system (CNS) anti-inflammatory effects.[8,9] When activated by deoxyribonucleic acid (DNA) damage, cytokine signaling, or other factors, PARPs consume NAD^+ to form branched ADP-ribose chains on target proteins.[10,11] The poly(ADP-ribose) polymers affect interactions between the modified protein and DNA, ribonucleic acid (RNA), and other proteins, including chromatin and pro-inflammatory transcription factors.[10,12–14] Mammalian cells contain several PARP family members, of which PARP-1 is the major species.[15,16] Macrophages and microglia that are genetically deficient in PARP-1 exhibit minimal nuclear factor-kappaB (NF-κB) activation, tumor necrosis factor alpha (TNFα) release, or induction of inducible nitric oxide synthase (iNOS) in response to pro-inflammatory stimuli.[2,17] Pharmacological inhibition of PARP activity similarly suppresses cytokine and nitric oxide release by microglia and macrophages.[2]

Independent of these anti-inflammatory actions, PARP inhibitors also have an acute neuroprotective effect stemming from their

[1]Department of Neurology University of California San Francisco, and San Francisco Veterans Affairs Medical Center; San Francisco, California.
[2]Department of Neurosurgery, Jinling Hospital, School of Medicine, Nanjing University, Nanjing, People's Republic of China.
[3]Department of Neurological Surgery University of California San Francisco, and San Francisco Veterans Affairs Medical Center; San Francisco, California.
[4]Programa de Pós Graduação em Ciências Biológicas: Bioquímica, UFRGS, Porto Alegre, Brazil; and Science Without Borders, CNPq, Brasilia, Brazil.
Current Address for K.-A.I: Anesthesiology Service, VA Palo Alto Health Care System, Palo Alto, California: Department of Anesthesiology, Perioperative and Pain Medicine, Stanford University School of Medicine, Stanford, California.

ability to slow the consumption of NAD^+ in cells with DNA damage.[18] Several studies have evaluated acute administration of PARP inhibitors in animal models of brain trauma and found generally positive results.[19–23] This neuroprotective effect, however, requires drug administration within very short time intervals after injury,[19] which limits clinical applicability. By contrast, inflammatory responses require several hours to become fully manifest and then continue for days. Given the efficacy of PARP inhibitors in suppressing brain inflammation, we aimed to determine whether a PARP inhibitor could improve long-term recovery when administered at clinically relevant time points after brain trauma.

The present study was designed as a pre-clinical efficacy study, using an orally absorbed PARP inhibitor (veliparib), long (eight-week) evaluation intervals, and pre-determined measures of cognitive and motor function. Rats were used to assess veliparib effects on histological and behavioral outcomes over eight weeks post-injury, and both rats and pigs were used to evaluate a range of veliparib doses on post-injury microglial activation. Veliparib (ABT-888; 2-((*R*)-2-Methylpyrrolidin-2-yl)-1*H*-benzimidazole-4-carboxamidename) inhibits PARP-1 and PARP-2 with K_is of 5.2 and 2.9 nmol/L, respectively, displays good CNS penetration, and is currently in phase II and III clinical trials for treatment of those with various forms of cancer.[24,25]

Methods

The studies were approved by the San Francisco Veterans Affairs Medical Center Animal Care and Use Committee. Male Long Evans rats (250–300 g; Simonsen Laboratories, CA) were housed on a reverse 12-h light/dark cycle with a restricted food diet (9 g/day) but free access to water. Castrated male Yorkshire swine, weight 23–28 kg, were obtained from Pork Power Farms (Turlock, CA) and maintained on a diet of Teklad Miniswine Diet 7037, with twice-daily feeding. Veliparib was obtained from Abbvie, Lake Bluff, IL. Other drugs and reagents were obtained from Sigma-Aldrich (St. Louis, MO) except where noted.

Rat studies

Rat controlled cortical impact (CCI). A CCI device (Pinpoint Precision Cortical Impactor, Hatteras Instruments, NC) was used to produce a unilateral CCI injury. Animals were anesthetized with isoflurane (5% for induction and 2.5% for the duration of the procedure; Abbott Laboratories, IL) and maintained at 37°C ± 0.5°C with a thermal mat throughout the surgical procedure. The anesthetized rats were placed in a stereotaxic frame with heads positioned to target the impact 3.0 mm left of bregma. A midline scalp incision and a circular craniotomy were made, and the dura was carefully opened with a scalpel. All studies used a 4 mm diameter impactor programmed to 1.5 m/sec velocity, 3.0 mm penetration depth, and 120 msec dwell time. After CCI, the operative site was closed with sutures, a subcutaneous injection of 6 mg/kg bupivacaine was administered, and the animals were maintained at 37°C for 30 min until they had recovered from anesthesia. Sham-operated controls were subjected to the same surgical procedures except the craniotomy and cortical impact. The perioperative mortality rate was 0 of 131 total.

Animal cohorts. A first cohort of 25 rats was used to establish the effective dose of veliparib as an anti-inflammatory agent in the brain. A second cohort of 57 rats was used to establish the effect of this dose on proinflammatory gene expression, axonal transport, and cell death in the dentate gyrus after CCI. A third cohort of 12 rats was used for long-term functional outcome studies, using 24 h between CCI and first drug dose. A fourth and fifth cohort of 12 rats each was used for long-term functional outcome studies, using 2 h between CCI and first drug dose. Of these, two rats necessitated euthanasia during the eight-week post-injury evaluation period. The fifth cohort received drug twice daily; all other cohorts received drug once daily. Results of the 4th and 5th cohorts were combined, because no difference was observed between once-daily and twice-daily dosing. Separately, 15 rats underwent CCI to establish the time course of axonal loss in the corpus callosum over 180 days after CCI.

Drug administration. Veliparib was prepared as a 20 mg/mL stock solution in physiologic saline and sterile-filtered. This stock solution was diluted subsequently for each dose employed such that the intraperitoneal injection volume was approximately 1 mL per rat (adjusted to account for small variations in rat weights). Sham CCI-treated rats and CCI-treated rats given 0 mg/kg veliparib in the dose-response studies received 1 mL injections of the sterile saline vehicle on the same dosing schedule as the rats receiving veliparib.

Gene expression studies. Rats were euthanized by anesthesia and decapitation at designated time points after CCI. The quadrant of brain containing the CCI was removed, and the necrotic area was discarded. A tissue sample immediately adjacent and inferior to the necrotic area was taken from each brain for analysis. Total RNA was extracted using the High Pure RNA Isolation kit (Roche) and immediately reverse transcribed to cDNA with a cDNA Synthesis Kit (Thermo Fisher). Samples were analyzed in triplicate. The primers were designed according to Pubmed GenBank and synthesized by Eurofins Genomics.

The primer sequences were as follows: Iba-1, f: TTAGAGA GGTGTCCAGTGGC r: CTCTGGCTCACAACTGCTTC; IL-1ß f: CGACAAAATACCTGTGGCCT r: TTCTTTGGGTATTGCTT GGG; TNF-α f: TCGTAGCAAACCACCAAGTG r: TTGTCTTT GAGATCCATGCC; MMP9, f: CCCTCTGCATGAAGACGACA r: CAGAAGGACCAGCAGTAGGG; MRC2, f: TGCGTCTTACT TCTCGGGG r: CCCAGGTTGAAGAGTCGGTT; SOCS3, f: GTC ACCCACAGCAAGTTTCC r: GCTGTCGCGGATAAGAAAGG.

Quantitative real-time polymerase chain reaction (PCR) analysis was performed with an Mx3000P system (San Diego, CA), using SYBR Green to measure double strand DNA content. A dissociation step was added at the end of the PCR to confirm the amplification of a single product. The transcript level of each gene was normalized to the GAPDH mRNA in the same sample using the $2^{-\Delta\Delta CT}$ method.[26]

Immunohistochemistry. Rats were anesthetized deeply with isoflurane, given a bilateral thoracotomy, and transcardially perfused with ice cold saline followed by 4% formaldehyde. Brains were post-fixed in 4% formaldehyde overnight at 4°C, cryoprotected in 20% sucrose for two days at 4°C, and frozen rapidly in dry ice. Serial 40 μm coronal sections were obtained using a cryostat. Four sets of 24 evenly spaced sections spanning the injured cortex and the hippocampus were collected from each brain. Degenerating cells were identified by Fluoro-Jade B (FJB) staining performed as described previously.[27,28]

Immunostaining was performed using goat polyclonal antibody to Iba-1 for microglia and macrophages (1:1000, Abcam, Cambridge, UK), rabbit polyclonal antibody to glial fibrillary acidic protein for astrocytes (GFAP; 1:1000, EMD Millipore, MA), mouse monoclonal antibody to NeuN for mature neurons (1:1000, EMD Millipore), mouse monoclonal antibody to nonphosphorylated neurofilaments (clone SMI-31R, 1:1000, Biolegend, NJ), and rabbit polyclonal antibody to amyloid precursor protein for axonal spheroids (APP; 1:500, Invitrogen, CA).

For antibodies visualized by the DAB method (Vector Laboratories, CA), sections were pre-treated with 0.3% hydrogen peroxide in phosphate-buffered saline (PBS) for 30 min. For APP, sections subsequently underwent antigen retrieval using pre-warmed (80°C)

sodium citrate buffer (pH 6.0) for 30 min. Sections remained in this buffer while cooling to room temperature. Incubations with all antibodies were made in blocking buffer containing 1% albumin, 2% normal serum. and 0.3% Triton X-100. Iba-1, SMI-31R, and NeuN antibody binding was imaged using fluorescent second antibodies and confocal microscopy (Zeiss LSM 510) with appropriate filter sets. GFAP and APP antibody binding was visualized by the DAB method, using biotin-conjugated second antibodies and the Vectastain Elite ABC reagent (Vector Laboratories).

Controls omitting primary antibody showed no detectable fluorescence and minimal background DAB staining under the conditions employed. Staining was performed concurrently for each group of sections compared with one another and photographed under identical conditions by an individual blinded to the experimental conditions.

Image analysis. In all data assessments, both the photography and image analysis were performed by observers who were blinded to the experimental conditions. Lesion cavity size was defined as the sum of the areas of absent hematoxylin and eosin staining on each section, multiplied by the distance between sections.[29] Iba-1 expression was evaluated in the lesioned cortex on three coronal sections per brain spaced 40 μm apart, in two regions each located 200 μm from the edge of the lesion (as defined by complete lack of NeuN staining; Fig. 1) for a total of six images per brain. Iba-1 expression level in each photographed area was calculated by multiplying the net area of Iba-1 staining by the mean intensity of Iba-1 staining within this area, using the NIH ImageJ program.

GFAP expression was evaluated in the ipsilateral dentate gyrus on two coronal sections per brain spaced 400 μm apart, three images per section. The percentage of the total image area covered by GFAP in each section was calculated using the ''area fraction'' feature in the National Institutes of Health (NIH) ImageJ program. APP accumulation in axonal spheroids was evaluated in the ipsilateral corpus callosal radiations in three coronal sections per brain spaced 400 μm apart, three images per section. Sections from control (uninjured) rats that had been fixed, stained, and photographed in parallel were used to establish a threshold for excluding nonspecific staining.

APP positive spheroids 1 μm in diameter or larger were quantified using the ''analyze particles'' feature of the NIH ImageJ program. Axonal loss was quantified in one image from each of three coronal sections per brain, spaced 400 μm apart, and taken at a magnification spanning the corpus callosum. The sections were immunostained for neurofilament and the relative number of axons in the corpus callosum was estimated using a Microcomputer Imaging Device (Imaging Research Inc.), with a point grid overlaid on $\times 40$ magnification images of the stained sections. The axon density was calculated by counting the number of grid points that fell on an axon, subtracting this value from the total number of grid points, and multiplying by 100 to express this as a percentage. This percentage was then multiplied by the dorsal-medial thickness of the corpus callosum to derive the relative number of axons.[30] The

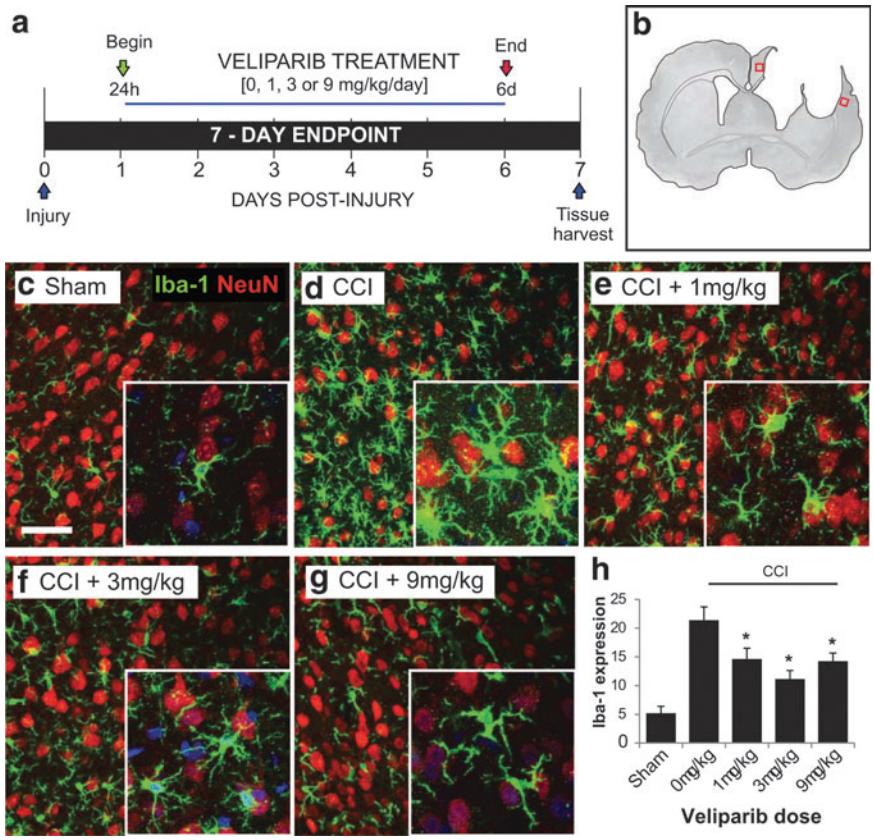

FIG. 1. Veliparib suppresses microglial activation in the rat brain. **(a)** Experimental design. **(b)** Representative coronal brain section through the area of maximum injury. Red boxes denote perilesional areas in which microglial activation was assessed. (**c–g**) Representative confocal images of microglia/macrophages in the perilesional area from rats treated with veliparib at the designated daily doses. Rat treated with sham controlled cortical impact (CCI) or 0 mg/kg veliparib received vehicle (saline) in place of veliparib. Iba-1 (green) identifies microglia/macrophages. DAPI (blue) identifies cell nuclei, with neuronal nuclei also labeled with NeuN (red). Scale bar = 50 μm. Inserts show microglial morphology at higher magnification. (**h**) Graph shows quantified Iba-1 expression in each treatment group ($n = 5$; $^*p < 0.05$ vs. CCI, 0 mg/kg veliparib).

number of FJB-positive cells was counted in the dentate gyrus ipsilateral to the lesion in three coronal sections spaced 320 μm apart. The mean number of FJB-positive neurons per section ipsilateral to CCI was used for statistical analyses.

Rat behavioral assessments

5-Choice Serial Reaction-Time Task (5-CSRTT). This is an operant conditioning paradigm to measure aspects of attentional and inhibitory control in rodents.[31] The animals were trained over 30–40 days before CCI to respond to brief flashes of light presented pseudo-randomly in one of five apertures with a nose-poke response in the correct spatial location. The rats were motivated by a food reward (45 mg; TestDiet, IN). The training and assessments were performed using a Bussey-Saksida Touch Screen Chamber for rodents (Campden Instruments) and ABET II touch software (Lafayette Instrument Company). Nose pokes in the wrong location were scored as errors; nose pokes before stimulus presentation were scored as premature responses; and failures to respond within 5 sec were scored as omissions. Each session terminated after 100 trials or 30 min, whichever came first. Rats were considered fully trained when they could correctly respond to a 0.7 sec light stimuli and when their accuracy was greater than 75% and omissions were fewer than 15% on two consecutive days. Training frequency was then reduced, and the rats were subjected to CCI or sham operation within the next 10 days.

Forelimb Use Asymmetry Test. Animals were placed in a clear plastic cylinder (diameter = 20 cm; height = 46 cm) and spontaneous exploratory behavior was recorded for 5 min. Slow motion video playback was used to determine the number of times the animal placed its left, right, or both forepaws against the side of the cylinder.[32] Results are reported as a percentage of the total paw placements made with the paw contralateral to injury.

Forelimb Dexterity Test. (Irvine, Beatties, and Bresnahan scale [IBB]): Rats were videoed while eating two differently shaped cereals (spherical and doughnut) of a consistent size. The videos were replayed in slow motion to assess features of forelimb use including joint position, object support, digit movement, and grasping technique.[33,34]

Elevated Plus Maze Anxiety Test. Each rat was placed in the center of a plus maze composed of two open arm and two closed arms. Rat location in the maze was tracked using the SMART video-tracking system (Panlab S.L.U, Spain) for 5 min and scored subsequently as described.[35]

Pig studies

Pig CCI. Pigs were acclimated for at least 5 days before operation and fasted for 12 h before the procedure. On the morning of the surgical procedure, they were sedated with ketamine/xylazine/glycopyrrolate and then anesthetized with 1.5–3.5% isoflurane in air as detailed previously.[36] A right femoral arterial line was inserted. Blood pressure, heart rate, echocardiography, oxygen saturation, end tidal carbon dioxide, and rectal temperature were monitored continuously using a Datex Engstrom AS/3 monitoring system. Arterial oxygen saturation was maintained at >98% and end tidal carbon dioxide at approximately 40 mm Hg.

A craniotomy was made targeting motor cortex, centered 14 mm anterior to bregma and 10 mm lateral to the sagittal suture. A Cortical Impactor (Hatteras Instruments) was used to create a CCI at these coordinates with speed 3.5 m/sec, depth 10 mm, and dwell time 400 msec. The long dwell time was used to increase the injury size that can be produced with the impactor on the relatively large pig brain. After closure of the craniotomy, wound margins were infiltrated with bupivacaine, and the anesthesia was discontinued. Sham-injury pigs underwent anesthesia and craniotomy, but not CCI.

Drug administration. Veliparib was mixed into corn syrup to prepare a stock concentration of 90 mg/mL. This stock was diluted as needed with corn syrup to provide doses of 1, 3, or 9 mg/kg and administered twice daily with meals in 3 mL corn syrup. Sham CCI-treated pigs and CCI-treated pigs given 0 mg/kg veliparib received 3 mL of the corn syrup vehicle only, twice daily with meals.

Pig immunohistochemistry. Pigs were sedated, deeply anesthetized with isoflurane, and euthanized by bilateral thoracotomy and perfusion with heparinized saline. Brains were removed, divided into three blocks, post-fixed in 4% buffered formaldehyde for 7 days, and cryoprotected with 20% sucrose. The brains were frozen and cut into 40 μm coronal sections spanning the lesion area. Immunostaining for microglia/macrophages was performed using goat polyclonal antibody to Iba-1 (1:1000, Abcam, Cambridge, UK) and visualized by the DAB method, using biotin-conjugated second antibodies and the Vectastain *Elite* ABC reagent (Vector Laboratories).

Because of the complex topology of the lesions and perilesional inflammation in the gyriform brains, a nonbiased method was used to quantify the area of increased Iba-1 immunoreactivity. Analysis was performed on three sections spaced 1 mm apart through the lesion epicenter. The NIH ImageJ program was used to quantify the area and intensity of Iba-1 immunoreactivity. The area of the lesion (A_L) was defined as the total area/section in which signal intensity was at least 30% greater than the mean intensity of signal from a region remote from injury. The increase in Iba-1 expression was calculated as $(I_L - I_B)$ X A_L, with I_L = mean Iba-1 intensity of lesion area, and I_B = mean intensity of the nonlesioned area (i.e., background). All sections used were stained concurrently and photographed under identical conditions by an observer who was blinded to the treatment groups.

Pig behavioral assessments

Bucket Memory Task. The tasks were modified from that of Alam and colleagues.[37] Before CCI, pigs were trained to discriminate between three white buckets, each painted with a different black pattern. All three buckets contained a food reward, but only one could be opened. Trials were performed twice per day, with five tests per trial. The pig was given one attempt to identify the correct bucket in each test, with the buckets rearranged between each test. When the pig attained an 80% success rate, trial frequency was reduced to once per day until CCI or sham operation to prevent over-training. Twice-daily trials were resumed on day two after CCI (or sham) surgical procedure, with the percent successful attempts recorded for each pig in each trial.

Novel object recognition test. Beginning on day two after CCI or sham operation, each pig was released into a testing area in which two T-shaped plastic pipes were hung, colored either white or black. There were four 3-min trials, two per day on two consecutive days. In the first three trials, the objects were the same color, and for the last trial, the color of one of the objects was different. The time spent in contact with each object was recorded, and the difference in time spent between the original object and the new object was calculated for each pig in this trial.

Gait assessment. Before CCI, pigs were trained to walk over a six-inch tall hurdle to a food reward while being filmed from the side to capture each hoof as it went over the hurdle. The pig was led across the hurdle 10 times in each trial. Pigs were considered fully trained when they avoided hoof contact with the hurdle greater than 90% of the time. Beginning on day two after CCI or sham operation, pigs were again led across the hurdle and assigned one point

for each hoof that touched the hurdle. Scores for each pig were summed over three trials performed on consecutive days.

Data analysis. Outcome measures were in each case evaluated by observers blinded to experimental conditions. Results are presented as mean ± standard error. Histology results were performed by one-way analysis of variance (ANOVA) followed by the Dunnett test for multiple comparisons against a common group, or by the Student-Newman-Keuls method for multiple pairwise comparisons. Behavioral data were analyzed using repeated measures ANOVA with Greenhouse-Geisser correction followed by the Tukey multiple comparison test.

Results

Veliparib dose-response studies

The rat CCI targeted the forelimb area of the sensorimotor cortex, and at the lesion epicenter the resulting cavity extended through the underlying corpus callosum into the caudate nucleus (Fig. 1). Immunostaining for the microglia/macrophage marker Iba-1 demonstrated a roughly four-fold increase in density of labeled cells in the perilesional area and showed them to have enlarged cell soma characteristic of the activated morphology.

We first evaluated veliparib over a range of doses to establish a dose that could suppress inflammation effectively after CCI. Veliparib (or saline vehicle) was administered intraperitoneally once per day beginning 24 h after CCI, and brains were harvested on day seven after injury (Fig. 1). Veliparib significantly reduced the microglial/macrophage activation at all doses tested, with no significant difference between the doses (Fig. 1c–h).

We also assessed effects of veliparib on neuronal death in the hippocampal dentate gyrus, a region that is anatomically remote from the CCI and susceptible to delayed death after brain trauma. Consistent with previous reports,[38,39] we observed scattered degenerating cells in this region seven days post-CCI, as identified with FJB (Fig. 2b,c). Rats treated with veliparib showed significantly reduced cell death, again with no significant difference between the different doses employed. The dentate gyrus also showed a marked increase in astrocyte GFAP expression (reactive astrocytosis) after CCI. The increase in GFAP expression was also attenuated by veliparib, with statistically significant effects observed in the 3 and 9 mg/kg treatment groups (Fig. 2d–g). Based on these results, we chose the 3 mg/kg dose for the subsequent studies.

Gene expression changes

To confirm veliparib efficacy on inflammatory responses, we evaluated drug effects on several inflammation-related gene products: IL-1ß, TNF-α, Iba-1, MRC2, MMP9, and SOCS3. Each of these mRNA species were increased in the perilesional tissue during the first few days after CCI (Fig. 3a). Rats treated with veliparib beginning 24 h after CCI showed attenuated increases in some, although not all of these gene products (Fig. 3b).

Effects on axonal injury and survival

We also evaluated the effect of veliparib on axonal injury and loss in the ipsilateral callosal radiations at seven days and eight weeks after CCI, given that inflammation may contribute to delayed axonal injury after traumatic brain injury.[40] At the seven-day time point, we assessed APP-positive axonal spheroids, which are a marker of impaired axonal transport. These were evident throughout the white matter tract and, surprisingly, were increased in rats treated with veliparib (Fig. 4). At the eight-week time point, we assessed the long-term survival of corpus callosum axons by quantitative analysis of neurofilament number. This assessment showed that axonal density was strikingly reduced in the CCI rats, to values less than 10% of sham-CCI–treated rats (Fig. 5). The number of axons surviving at this time point was neither increased nor decreased in the rats that had been treated with veliparib. In a separate study, groups of rats evaluated at time points between seven and 180 days post-injury confirmed that the axonal loss was a delayed response to injury (Fig. 5e).

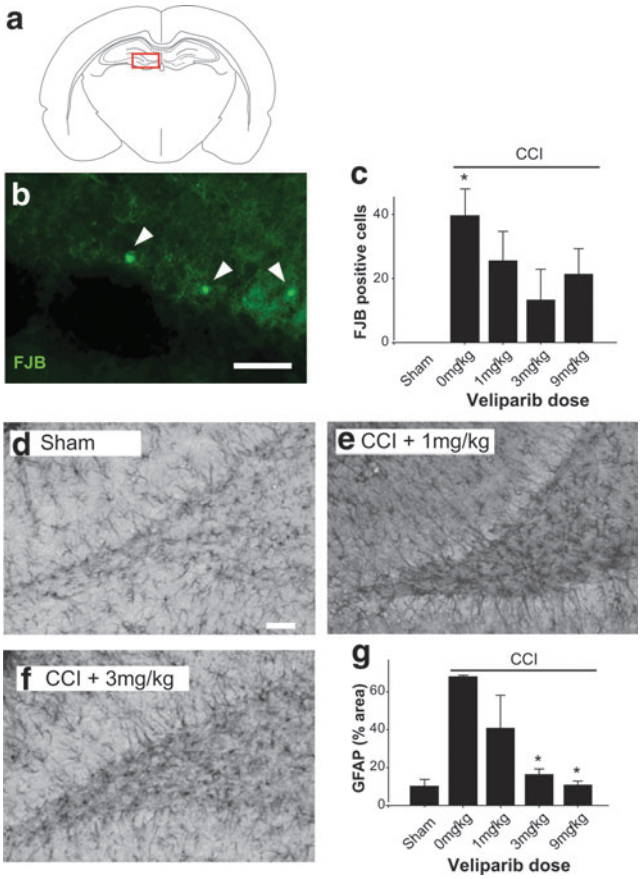

FIG. 2. Veliparib reduces astrocyte activation and cell death in hippocampal dentate gyrus after controlled cortical impact (CCI). (**a**) Box in schematic shows location in which these were assessed. Note the coronal plane of analysis is posterior to the injury site. (**b**) Degenerating cells identified by Fluoro-Jade B (FJB) staining seven days after CCI; scale bar = 50 μm. (**c**) Average number of FJB-positive cells per section in each treatment group ($n = 5$; $^*p < 0.05$ vs. sham CCI. (**d–f**) Expression of glial fibrillary acidic protein (GFAP, black) in representative sections from rats treated as indicated. Scale bar = 100 μm. (**g**) Graph quantifies area of GFAP staining in each treatment group ($n = 5$; $^*p < 0.05$ vs. CCI, 0 mg/kg veliparib).

Long-term functional outcome studies

Rats were divided arbitrarily into sham operation, CCI, or CCI plus veliparib treatment groups. All groups received 1 mL intraperitoneal injections of either veliparib (3 mg/kg) or vehicle only (saline) once per day for 12 days beginning 24 h after operation. Rats were evaluated for motor and cognitive deficits at multiple

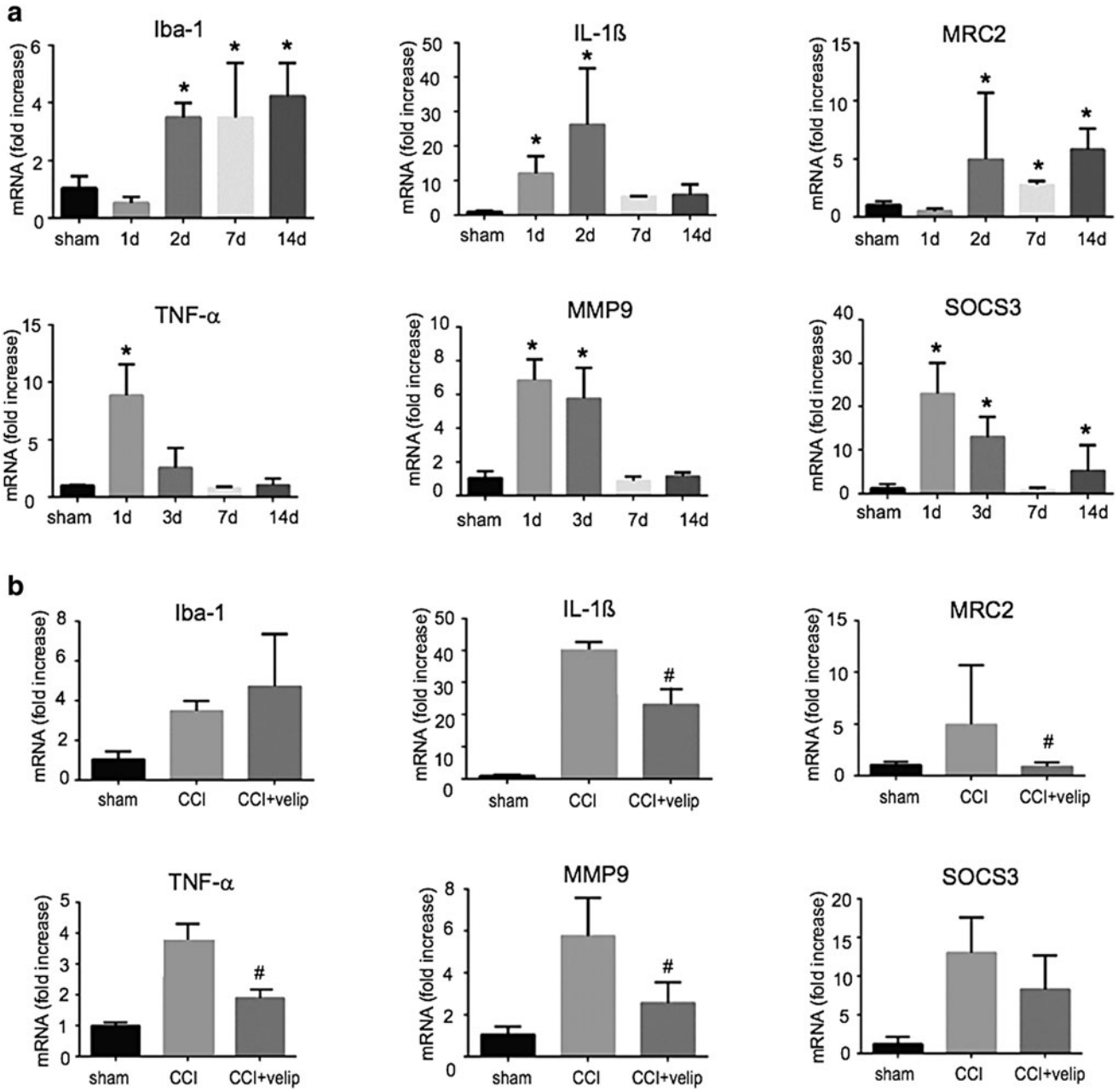

FIG. 3. Gene expression in perilesional brain tissue. (**a**) Relative increase in mRNA levels of designated gene products over two weeks after controlled cortical impact (CCI). (**b**) Effect of 3 mg/kg veliparib on expression levels of these genes at three days after CCI. Veliparib was administered daily beginning 24 h after CCI. Rat treated with sham CCI or 0 mg/kg veliparib received vehicle (saline) in place of veliparib. $n = 4$ for each determination; $*p < 0.05$ vs. sham CCI (ANOVA and Dunnett test); $\#p < 0.05$ vs. CCI (Student t test).

time points until eight weeks after CCI, at which time brains were harvested for histological assessments (Fig. 6a). The CCI -induced cavity size was not affected by veliparib (Fig. 6b), as expected with the delayed dosing protocol.

Motor function, as evaluated by the forelimb use asymmetry test and the IBB forelimb dexterity tests, showed significant deficits after CCI. These deficits improved over the initial three weeks after injury and then plateaued. Veliparib-treated rats did no better than vehicle-treated rats on the forelimb asymmetry test and did statistically worse than vehicle-treated rats on the IBB test (Fig. 6c,d). Attention and executive function, as evaluated by the 5-CSRTT test, showed deficits that gradually resolved over 4–6 weeks after CCI. The rate of resolution was not influenced by veliparib treatment (Fig. 6e,f).

Long-term outcome studies with 2 h delay to treatment

Given that no behavioral benefit was observed with the 24 h delay to treatment, we considered the possibility that processes initiated before this time point may be crucial to the long-term functional outcomes. We therefore evaluated rats treated with only a 2 h delay between CCI and first dose of veliparib (Fig. 7a). Lesion cavity size was again unaffected by veliparib (Fig. 7b). The number of corpus callosum axons surviving at the eight-week time point

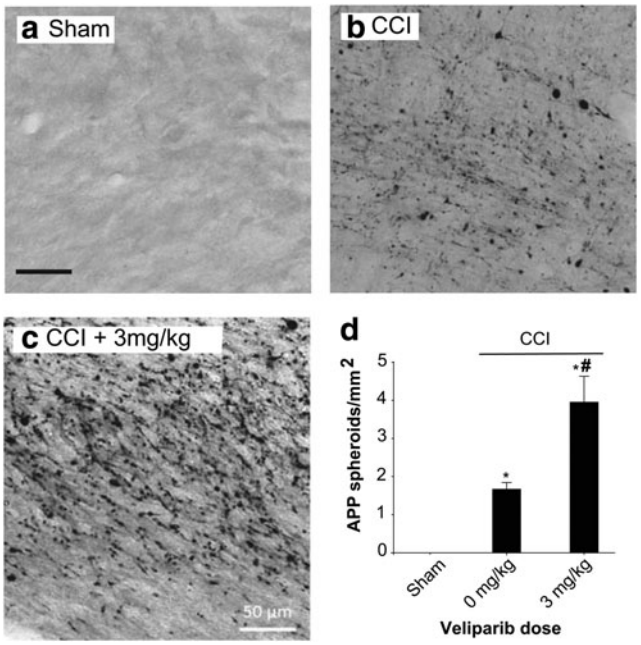

FIG. 4. Veliparib increased accumulation of amyloid precursor protein (APP) in axonal spheroids in callosal radiations. (**a–c**) APP accumulation (black) in representative sections from rats treated as indicated. Scale bar = 50 μm. (**d**) Graph quantifies APP spheroids in each treatment group. $n = 5$; $^{*}p < 0.05$ vs. sham, $^{\#}p < 0.05$ vs. controlled cortical impact (CCI), 0 mg/kg veliparib.

was also unaffected by veliparib (Fig. 7c). Motor function, as evaluated by the forelimb asymmetry test and the IBB forelimb dexterity tests, again showed significant deficits after CCI that resolved partially over the initial three weeks after injury. The rates and extent of motor recovery were unaffected by veliparib treatment (Fig. 7d,e). Attention and executive function, as evaluated by the 5-CSRTT test, showed deficits that resolved gradually after CCI and were not significantly affected by veliparib treatment (Fig. 7f,g).

In addition, we evaluated rats with the elevated plus maze to assess anxiety-like behavior, on day 14 and day 56 after injury. At the 14 day time point, the studies showed a trend toward increased latency in movement into open arms of the maze and increased time spent in the closed arms of the maze that were both attenuated by veliparib, but these effects were not significant after accounting for multiple comparisons (Fig. 7h,i). A separate analysis of the functional outcome measures using aggregated data from studies using both the 2 h and 24 h delay-to-treatment intervals (combined $n = 10$–12 per group) showed no statistically significant effect on veliparib on any of the functional outcome measures (Supplementary Fig. 1).

Pig studies

The CCI produced a lesion of relatively modest size relative to the overall pig brain (Fig. 8a,b). Immunostaining for Iba-1 to label microglia/macrophages in the perilesional cortex revealed a large increase in labeled cells and showed them to have enlarged cell

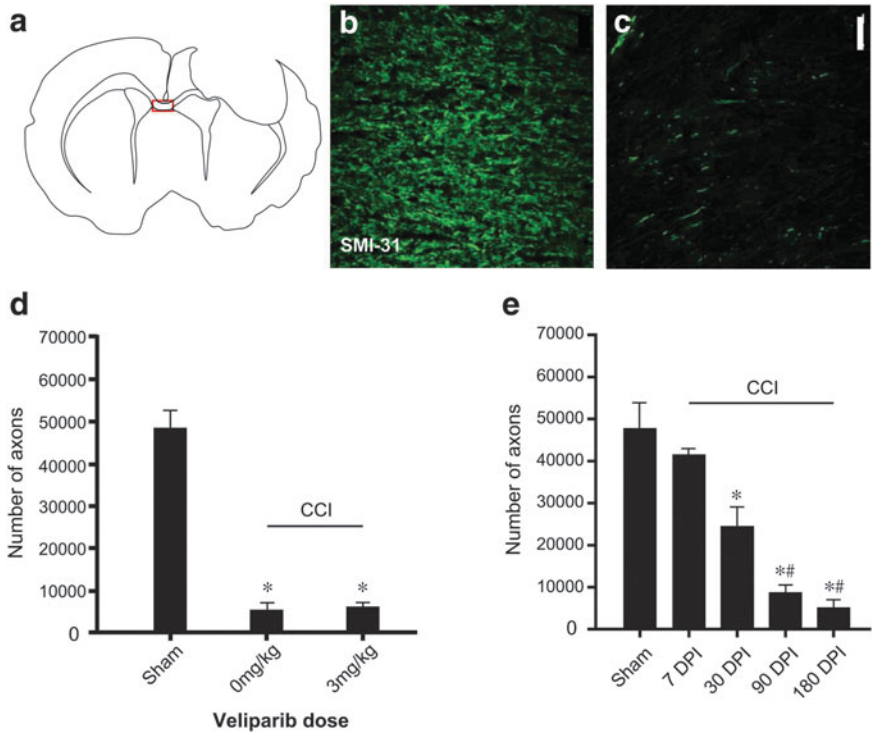

FIG. 5. Veliparib did not reduce axonal loss in corpus callosum assessed eight weeks later. (**a**) Location of region sampled for axonal density. Axons identified by neurofilament immunostaining (SMI-31, green) in the corpus callosum from **(b)** sham and **(c)** controlled cortical impact (CCI)-treated rats eight weeks after operation. Scale bar = 10 μm. **(d)** Quantified axonal survival ($n = 5$; $^{*}p < 0.01$ vs. sham). (**e**) Extended time course of callosal axon loss, seven to 180 days post-injury (DPI); $n = 3$; $^{*}p < 0.01$ vs. sham; $^{\#}p < 0.01$ vs. seven days post-injury.

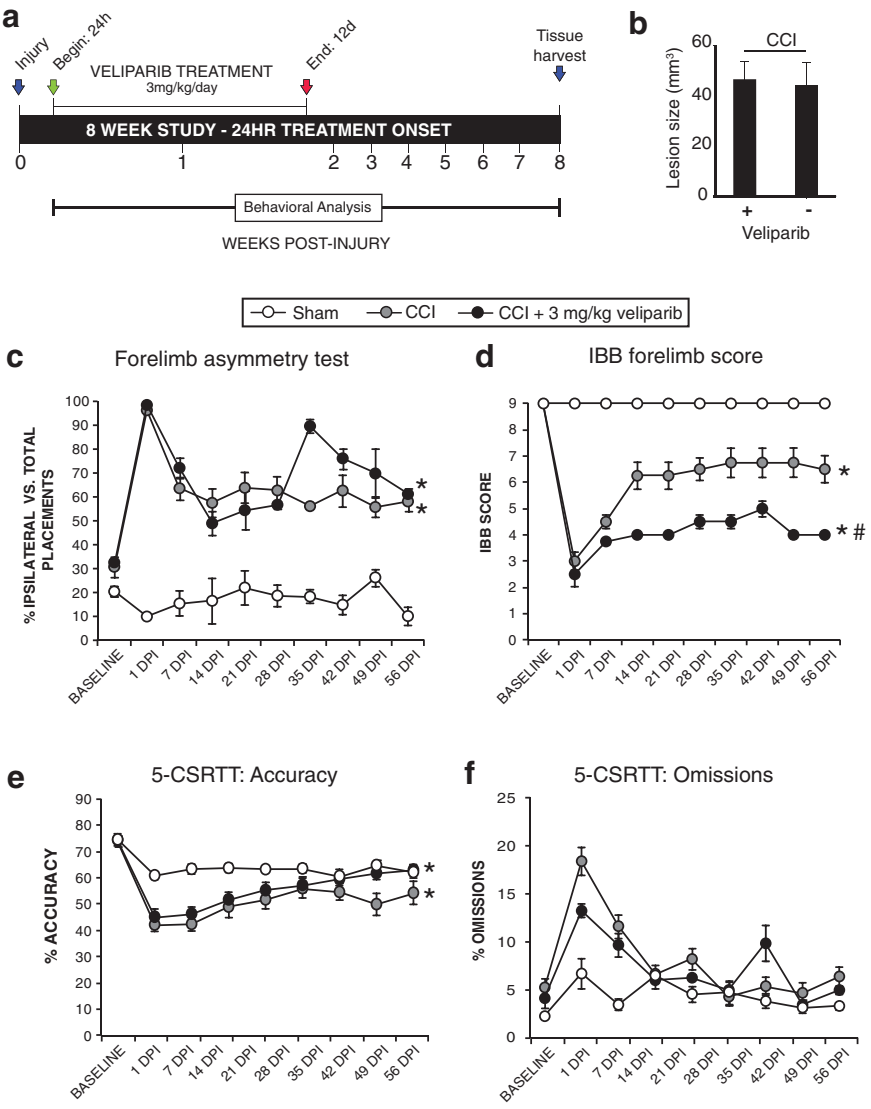

FIG. 6. Effects of veliparib initiated 24 h post-injury on motor function and attentional control 0–56 days post-injury (DPI). **(a)** Experimental design. **(b)** Lesion volumes measured eight weeks after controlled cortical impact (CCI) showed no effect on cavity volume ($n=4$). (**c**) Forelimb asymmetry test (*$p<0.01$ vs. sham). (**d**) Irvine, Beatties, Bresnahan (IBB) forelimb score (*$p<0.01$ vs. sham, $^{\#}p<0.01$ vs. CCI, no veliparib. **(e, f)** 5-Choice serial reaction time task (5-CSRTT) accuracy and omissions (*$p<0.01$ vs. sham). $n=4$ for each treatment group.

soma characteristic of the activated morphology (Fig. 8). The efficacy of veliparib in suppressing microglial/macrophage activation was assessed in pigs given doses of 0–9 mg/kg orally, twice per day, beginning 24 h after CCI or sham operation and continued for seven days ($n=5$ per group). Veliparib significantly reduced microglial/macrophage activation at all doses evaluated, with no significant difference between the doses (Fig. 8).

Pigs evaluated with the bucket memory test showed a modest but nonsignificant impairment on day two after CCI ($n=5$ CCI, $n=5$ sham; $p=0.08$), but all pigs were back to pre-injury performance levels by day three. The pigs likewise showed no impairments by the novel object recognition or gait tests by day three after surgery.

Discussion

These studies showed that the PARP inhibitor veliparib can effectively reduce the accumulation of activated microglia/macrophages and attenuate pro-inflammatory gene expression in the perilesional cortex after CCI. These anti-inflammatory effects were observed with a delay-to-treatment time of up to 24 h, over a range of doses, and in both rats and pigs. Despite these effects, however, long-term behavioral outcomes were not significantly improved in the veliparib-treated animals.

The anti-inflammatory effects observed with veliparib are concordant with previous studies using PARP inhibitors.[2,14,41–43,47–49] We evaluated expression of a pre-selected group of inflammation-associated genes to confirm that effects were mediated at the transcriptional level and found significant reductions in IL-1ß, TNF-α, and MMP9 gene expression. This pattern is consistent with the established effects of PARP inhibitors on NF-kB transcription factor activity.[13,41] The perilesional tissue samples taken for these assessments included mRNA from both microglia and nonmicroglial cell types, and consequently gene expression changes in the nonmicroglial cell types may contribute to (or dilute) the effects

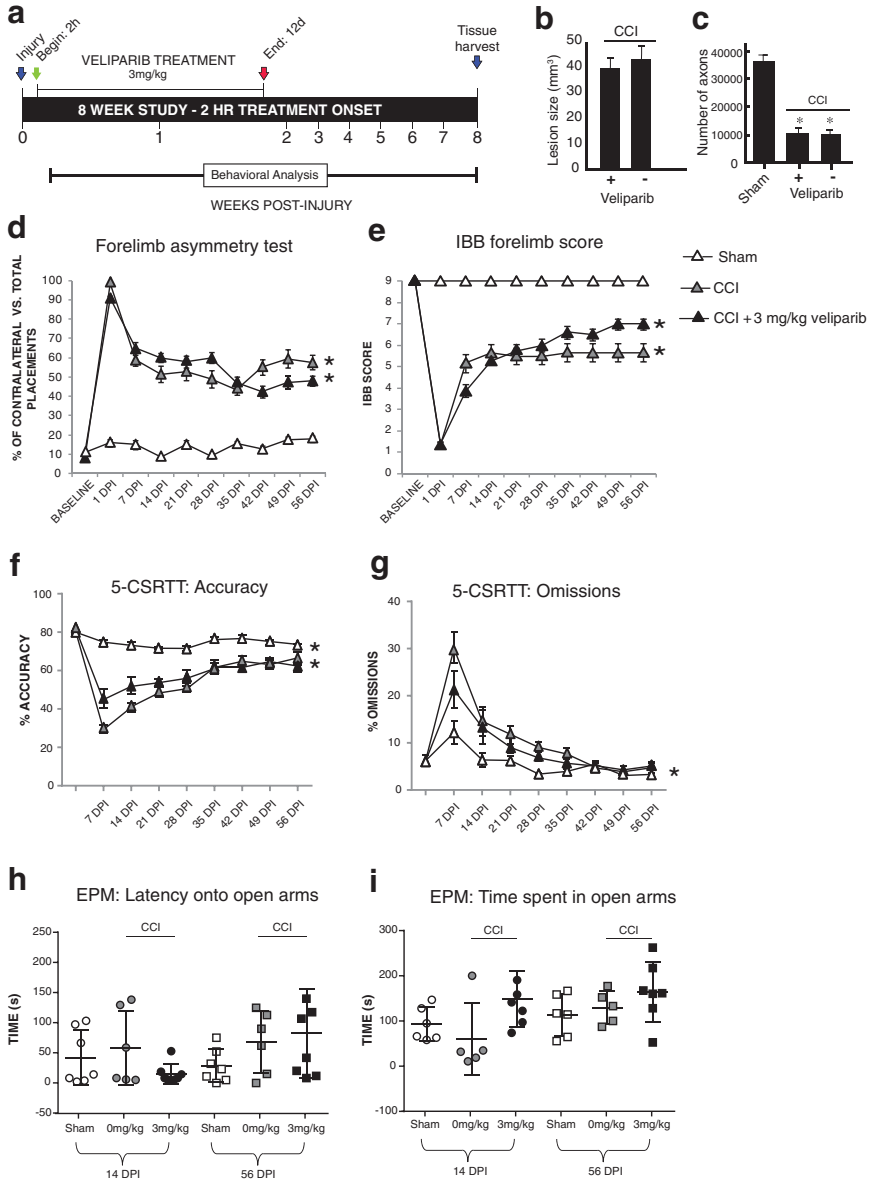

FIG. 7. Effects of veliparib initiated 2 h post-injury on motor function and attentional control 0–56 days post-injury (DPI). (**a**) Experimental design. **(b)** No effect of veliparib on lesion size 56 days post-injury ($n = 6$–8). **(c)** No effect of veliparib on callosal axon loss. (**d**) Forelimb asymmetry test ($n = 6$-8, $^*p < 0.01$ vs. sham). (**e**) Irvine, Beatties, Bresnahan (IBB) forelimb score ($n = 6$-8, $^*p < 0.01$ vs. sham). **(f, g)** 5-Choice serial reaction time task (5-CSRTT) accuracy and omissions ($n = 6$-8, $^*p < 0.01$ vs. sham). **(h, i)** Elevated plus maze (EPM) latency to enter open arms and time spent in open arms ($n = 6$–8). Total distance traveled was not affected by treatment conditions (not shown). In all outcome measures, comparisons between veliparib and vehicle-treated rats showed no significant differences.

observed. Veliparib did not significantly reduce Iba-1 mRNA levels, despite its robust effect on Iba-1 protein expression. Discordances between changes in mRNA and protein levels of Iba-1 and other inflammatory or cell-surface markers are recognized (e.g. [47,48]) and may reflect changes in post-transcriptional mRNA processing.[49]

In addition to reduced microglial activation, veliparib-treated rats showed reduced astrocytosis and a reduced number of degenerating cells in the hippocampal dentate gyrus. The degenerating cells, identified by FJB staining, are likely neurons, given that neurons in this structure are susceptible to remote effects of trauma[39] and FJB has specificity for degenerating neurons in most settings.[27,28] Cell-type specific markers, however, are degraded in degenerating cells by day seven after injury, thus precluding definitive identification of cell type. Assessment at the seven-day time point may also have missed neurons that died very soon after CCI. Nevertheless, the observation that veliparib administered 24 h after CCI reduced the number of degenerating cells and the accompanying astrocyte activation supports the idea that these may be delayed effects of inflammation.

Veliparib treatment did not affect lesion cavity size. This was an expected result, because the cavity induced by CCI results primarily from the mechanical disruption of cells and vasculature that occurs immediately with impact. By contrast, the axonal loss induced by CCI can be very delayed, as illustrated by the present findings (Fig. 5e). Although inflammation has been proposed as a mechanism driving delayed axonal degeneration,[40,48,50–53] the

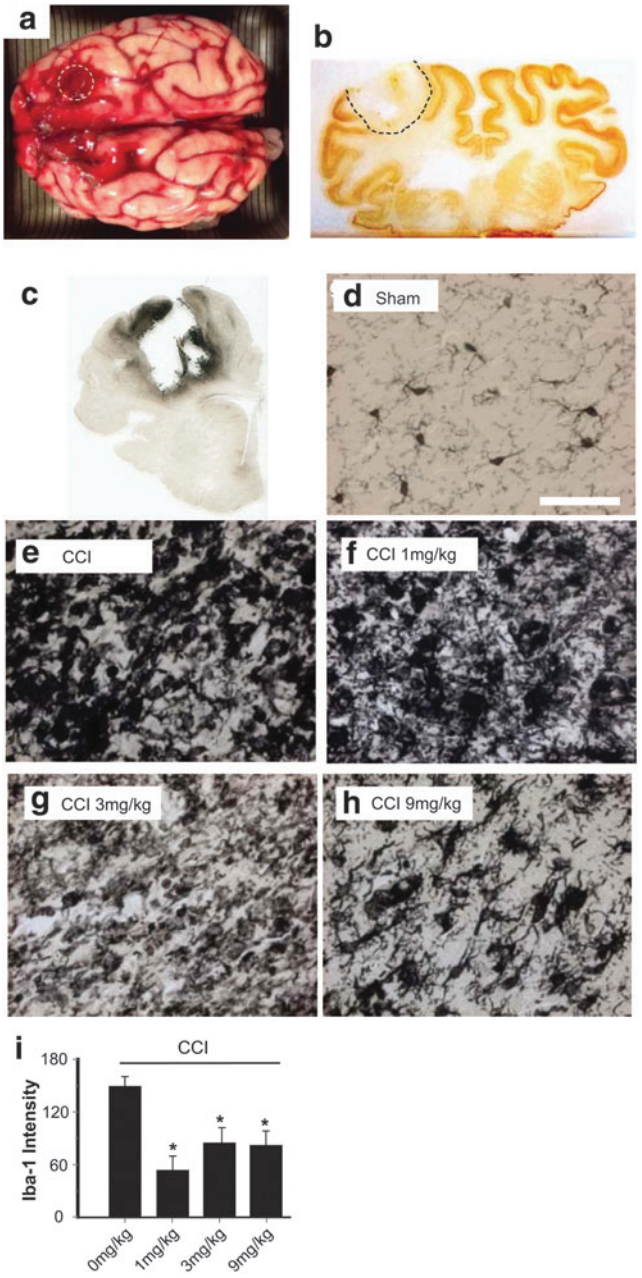

FIG. 8. Veliparib reduces controlled cortical impact (CCI)-induced microglial activation in pig brain. (**a**) Photograph of pig brain surface showing size and location of CCI. (**b**) NeuN-stained coronal section through epicenter of CCI cavity (56 days post-injury). (**c**) Section through injured hemisphere harvested seven days after CCI showing increased Iba-1 immunostaining (black) around the lesion margins. (**d–h**) representative photomicrographs from each of the treatment conditions. Veliparib (or vehicle) was administered orally, twice daily at the designated dose, beginning 24 h after CCI. Scale bar = 20 μm. (**i**) Quantified Iba-1 expression. $n = 5$ at each veliparib concentration; $^*p < 0.05$ vs. CCI, 0 mg/kg veliparib.

12-day treatment with veliparib did not attenuate the axonal loss observed here.

Inflammation has also been suggested as a cause of axonal transport impairment after brain trauma. Accordingly, we evaluated a marker of impaired axonal transport, APP-containing spheroids, at seven days after CCI to determine whether this was reduced by veliparib treatment. Surprisingly, veliparib caused a significant increase in spheroid formation. This increase was not associated with a long-term increase (or decrease) in axonal survival, and so this significance of the increase in APP-containing spheroids at the early time point is uncertain. It is possible that spheroid formation does not correlate with later axonal demise, or that its time course is simply accelerated or slowed by veliparib with no net change in extent. Previous studies on the role of PARP in axonal survival and regeneration have yielded conflicting results[54–56] and did not evaluate axonal transport or employ delayed treatment with PARP inhibitor.

The motor outcome measures employed here have been validated previously in the rat CCI model. Our present observations with the IBB forelimb dexterity test showed gradual but incomplete resolution of impairment, a pattern that should permit detection of increased or accelerated recovery. Cognitive performance was assessed with the 5-CSRTT, which is designed to measure visuospatial attention and impulse control.[31] This test has not been reported previously in studies of traumatic brain injury, but it provides a useful assessment of impulsivity and disrupted attentional control, both of which are salient sequelae of human brain trauma. We found that accuracy and omissions measured by this test were both increased after CCI, and both gradually improved to baseline over six weeks of testing. The eventual complete recovery obviated the possibility of detecting a drug effect on ultimate outcome, but the absence of any accelerated recovery argues against a drug effect. A previous study using the PARP inhibitor INH2BP reported impaired learning in rats being treated at high doses[21]; however, in the present study, veliparib was administered for only the initial 12 days of the eight-week observational period.

It is unlikely that our study was insufficiently powered to detect a biologically relevant effect of veliparib because the aggregate n for the functional outcome studies was 10-12 for both the drug-treated and control groups (Supplementary Fig. 1). Several authors have commented on the need for long-term follow-up intervals and predetermined end-points to increase the rigor of pre-clinical studies.[57] The study was designed with these considerations in mind, and this may have prevented false positive observations. It is also possible that effects of veliparib or other anti-inflammatory agents could be more evident after trauma with greater severity or vascular damage (and greater inflammatory response), or with a longer drug treatment course.

We used a 12-day treatment interval based on results of a previous PARP inhibitor study that showed no rebound inflammation after this interval, and positive results on short-term behavioral measures.[24] Nevertheless, even short-term local or systemic anti-inflammatory effects carry increasing risk of interfering with tissue remodeling and other factors required for recovery after brain injury.[58]

By one measure, the IBB forelimb dexterity test, rats treated with veliparib beginning 24 h after injury recovered less completely than rats treated with vehicle only. This negative effect, however, was not observed in the rats treated at 2 h after injury, with data aggregated across the treatment conditions, or with any other functional outcome measure. This observation may be a statistical outlier (Type 1 statistical error), the occurrence of which would not be unexpected given that the study as a whole included more than 60 outcome comparisons.

An over-reliance on rodent models may be a factor limiting the extent to which experimental advances in brain trauma have translated to clinical successes.[59] Our study design intended parallel studies in rats and pigs, but the absence of significant functional impairment in the pig CCI precluded assessment of drug

effect in that species. The lack of functional impairment in the pig may reflect either the lesser injury severity (CCI cavity relative to total brain size), or less sensitive functional assessments. There is a paucity of established approaches and normative data for pig functional assessment, particularly for measures of motor function, and the present descriptions may help address this gap. Importantly, the studies using pigs did demonstrate a robust suppression of perilesional microglial activation by veliparib. This is significant because of concerns that immune responses may have species-specific aspects (particularly in rodents) that limit extrapolation of experimental findings to human disease.[60]

Inflammation remains an attractive therapeutic target for brain trauma given the known cytotoxic effects of inflammation and the relatively long ''window of opportunity'' conferred by the many hours required for this response to develop fully. Results of the present study show that veliparib can potently and effectively suppress microglial activation after brain trauma, with a delay-to-treatment interval of at least 24 h. The absence of a robust functional improvement in the treated cohorts, however, underscores the complexities in translating an anti-inflammatory effect to clinically relevant outcomes.

Acknowledgments

This work was supported by a grant from the U.S. Dept. of Defense (W81XWH-13-2-0091) and by the Dept. of Veterans Affairs. We thank Autumn Sorrels (UCSF) for advice with the pig behavioral studies, and Preeti Mann, Anna Conti, Peter Swanson, and Owen Jansen for technical assistance.

Author Disclosure Statement

No competing financial interests exist.

References

1. Russo, M.V. and McGavern, D.B. (2016). Inflammatory neuroprotection following traumatic brain injury. Science 353, 783–785.
2. Kauppinen, T.M. and Swanson, R.A. (2005). Poly(ADP-ribose) polymerase-1 promotes microglial activation, proliferation, and matrix metalloproteinase-9-mediated neuron death. J. Immunol. 174, 2288–2296.
3. Chao, C.C., Hu, S., Molitor, T.W., Shaskan, E.G., and Peterson, P.K. (1992). Activated microglia mediate neuronal cell injury via a nitric oxide mechanism. J. Immunol. 149, 2736–2741.
4. Faden, A.I. (1993). Experimental neurobiology of central nervous system trauma. Crit. Rev. Neurobiol. 7, 175–186.
5. Hu, X., Liou, A.K., Leak, R.K., Xu, M., An, C., Suenaga, J., Shi, Y., Gao, Y., Zheng, P., and Chen, J. (2014). Neurobiology of microglial action in CNS injuries: receptor-mediated signaling mechanisms and functional roles. Prog. Neurobiol. 119-120, 60–84.
6. Chen, Y., Won, S.J., Xu, Y. and Swanson, R.A. (2014). Targeting microglial activation in stroke therapy: pharmacological tools and gender effects. Curr. Med. Chem. 21, 2146–2155.
7. Kochanek, P.M., Jackson, T.C., Ferguson, N.M., Carlson, S.W., Simon, D.W., Brockman, E.C., Ji, J., Bayir, H., Poloyac, S.M., Wagner, A.K., Kline, A.E., Empey, P.E., Clark, R.S., Jackson, E.K., and Dixon, C.E. (2015). Emerging therapies in traumatic brain injury. Semin. Neurol. 35, 83–100.
8. Weltin, D., Picard, V., Aupeix, K., Varin, M., Oth, D., Marchal, J., Dufour, P., and Bischoff, P. (1995). Immunosuppressive activities of 6(5H)-phenanthridinone, a new poly(ADP-ribose)polymerase inhibitor. Int. J. Immunopharmacol. 17, 265–271.
9. Haddad, M., Rhinn, H., Bloquel, C., Coqueran, B., Szabo, C., Plotkine, M., Scherman, D., and Margaill, I. (2006). Anti-inflammatory effects of PJ34, a poly(ADP-ribose) polymerase inhibitor, in transient focal cerebral ischemia in mice. Br. J. Pharmacol. 149, 23–30.
10. Gibson, B.A. and Kraus, W.L. (2012). New insights into the molecular and cellular functions of poly(ADP-ribose) and PARPs. Nat. Rev. Mol. Cell Biol. 13, 411–424.
11. Vuong, B., Hogan-Cann, A.D.J., Alano, C.C., Stevenson, M., Chan, W.Y., Anderson, C.M., Swanson, R.A., and Kauppinen, T.M. (2015). NF-κB transcriptional activation by TNFα requires phospholipase C, extracellular signal-regulated kinase 2 and poly(ADP-ribose) polymerase-1. J. Neuroinflammation 12, 229.
12. Bai, P. and Virag, L. (2012). Role of poly(ADP-ribose) polymerases in the regulation of inflammatory processes. FEBS Lett. 586, 3771–3777.
13. Ha, H.C., Hester, L.D., and Snyder, S.H. (2002). Poly(ADP-ribose) polymerase-1 dependence of stress-induced transcription factors and associated gene expression in glia. Proc. Natl. Acad. Sci. U. S. A. 99, 3270–3275.
14. Martinez-Zamudio, R.I. and Ha, H.C. (2014). PARP1 enhances inflammatory cytokine expression by alteration of promoter chromatin structure in microglia. Brain Behav. 4, 552–565.
15. Phulwani, N.K. and Kielian, T. (2008). Poly (ADP-ribose) polymerases (PARPs) 1-3 regulate astrocyte activation. J. Neurochem. 106, 578–590.
16. Kamboj, A., Lu, P., Cossoy, M.B., Stobart, J.L., Dolhun, B.A., Kauppinen, T.M., de Murcia, G., and Anderson, C.M. (2013). Poly(ADP-ribose) polymerase 2 contributes to neuroinflammation and neurological dysfunction in mouse experimental autoimmune encephalomyelitis. J. Neuroinflammation 10, 49.
17. Oliver, F.J., Menissier-de Murcia, J., Nacci, C., Decker, P., Andriantsitohaina, R., Muller, S., de la Rubia, G., Stoclet, J.C., and de Murcia, G. (1999). Resistance to endotoxic shock as a consequence of defective NF-kappaB activation in poly (ADP-ribose) polymerase-1 deficient mice. EMBO J. 18, 4446–4454.
18. Alano, C.C., Garnier, P., Ying, W., Higashi, Y., Kauppinen, T.M., and Swanson, R.A. (2010). NAD+ depletion is necessary and sufficient for poly(ADP-ribose) polymerase-1-mediated neuronal death. J. Neurosci. 30, 2967–2978.
19. LaPlaca, M.C., Raghupathi, R., Verma, A., Pieper, A.A., Saatman, K.E., Snyder, S.H., and McIntosh, T.K. (1999). Temporal patterns of poly(ADP-ribose) polymerase activation in the cortex following experimental brain injury in the rat. J. Neurochem. 73, 205–213.
20. Whalen, M.J., Clark, R.S., Dixon, C.E., Robichaud, P., Marion, D.W., Vagni, V., Graham, S.H., Virag, L., Hasko, G., Stachlewitz, R., Szabo, C., and Kochanek, P.M. (1999). Reduction of cognitive and motor deficits after traumatic brain injury in mice deficient in poly(ADP-ribose) polymerase. J. Cereb. Blood Flow Metab. 19, 835–842.
21. Satchell, M.A., Zhang, X., Kochanek, P.M., Dixon, C.E., Jenkins, L.W., Melick, J., Szabo, C., and Clark, R.S. (2003). A dual role for poly-ADP-ribosylation in spatial memory acquisition after traumatic brain injury in mice involving NAD+ depletion and ribosylation of 14-3-3gamma. J. Neurochem. 85, 697–708.
22. Besson, V.C., Croci, N., Boulu, R.G., Plotkine, M., and Marchand-Verrecchia, C. (2003). Deleterious poly(ADP-ribose)polymerase-1 pathway activation in traumatic brain injury in rat. Brain Res. 989, 58–66.
23. Clark, R.S., Vagni, V.A., Nathaniel, P.D., Jenkins, L.W., Dixon, C.E., and Szabo, C. (2007). Local administration of the poly(ADP-ribose) polymerase inhibitor INO-1001 prevents NAD+ depletion and improves water maze performance after traumatic brain injury in mice. J. Neurotrauma 24, 1399–1405.
24. Donawho, C.K., Luo, Y., Luo, Y., Penning, T.D., Bauch, J.L., Bouska, J.J., Bontcheva-Diaz, V.D., Cox, B.F., DeWeese, T.L., Dillehay, L.E., Ferguson, D.C., Ghoreishi-Haack, N.S., Grimm, D.R., Guan, R., Han, E.K., Holley-Shanks, R.R., Hristov, B., Idler, K.B., Jarvis, K., Johnson, E.F., Kleinberg, L.R., Klinghofer, V., Lasko, L.M., Liu, X., Marsh, K.C., McGonigal, T.P., Meulbroek, J.A., Olson, A.M., Palma, J.P., Rodriguez, L.E., Shi, Y., Stavropoulos, J.A., Tsurutani, A.C., Zhu, G.D., Rosenberg, S.H., Giranda, V.L., and Frost, D.J. (2007). ABT-888, an orally active poly(ADP-ribose) polymerase inhibitor that potentiates DNA-damaging agents in preclinical tumor models. Clin. Cancer Res. 13, 2728–2737.
25. Wagner, L.M. (2015). Profile of veliparib and its potential in the treatment of solid tumors. Onco. Targets Ther. 8, 1931–1939.
26. Livak, K.J. and Schmittgen, T.D. (2001). Analysis of relative gene expression data using real-time quantitative PCR and the 2(-Delta Delta C(T)) Method. Methods 25, 402–408.
27. Schmued, L.C. and Hopkins, K.J. (2000). Fluoro-Jade B: a high affinity fluorescent marker for the localization of neuronal degeneration. Brain Res. 874, 123–130.
28. Suh, S.W., Gum, E.T., Hamby, A.M., Chan, P.H., and Swanson, R.A. (2007). Hypoglycemic neuronal death is triggered by glucose reperfusion and activation of neuronal NADPH oxidase. J. Clin. Invest. 117, 910–918.

29. Swanson, R.A., Morton, M.T., Tsao-Wu, G., Savalos, R.A., Davidson, C., and Sharp, F.R. (1990). A semiautomated method for measuring brain infarct volume. J. Cereb. Blood Flow Metab. 10, 290–293.
30. Irvine, K.A. and Blakemore, W.F. (2008). Remyelination protects axons from demyelination-associated axon degeneration. Brain 131, 1464–1477.
31. Robbins, T.W. (2002). The 5-choice serial reaction time task: behavioural pharmacology and functional neurochemistry. Psychopharmacology (Berl) 163, 362–380.
32. Liu, Y., Kim, D., Himes, B.T., Chow, S.Y., Schallert, T., Murray, M., Tessler, A., and Fischer, I. (1999). Transplants of fibroblasts genetically modified to express BDNF promote regeneration of adult rat rubrospinal axons and recovery of forelimb function. J. Neurosci. 19, 4370–4387.
33. Irvine, K.A., Ferguson, A.R., Mitchell, K.D., Beattie, S.B., Beattie, M.S., and Bresnahan, J.C. (2010). A novel method for assessing proximal and distal forelimb function in the rat: the Irvine, Beatties and Bresnahan (IBB) forelimb scale. J. Vis. Exp. 46.
34. Irvine, K.A., Ferguson, A.R., Mitchell, K.D., Beattie, S.B., Lin, A., Stuck, E.D., Huie, J.R., Nielson, J.L., Talbott, J.F., Inoue, T., Beattie, M.S., and Bresnahan, J.C. (2014). The Irvine, Beatties, and Bresnahan (IBB) Forelimb Recovery Scale: an assessment of reliability and validity. Front. Neurol. 5, 116.
35. Pellow, S., Chopin, P., File, S.E., and Briley, M. (1985). Validation of open:closed arm entries in an elevated plus-maze as a measure of anxiety in the rat. J. Neurosci. Methods 14, 149–167.
36. Odland, R.M., Venugopal, S., Borgos, J., Coppes, V., McKinney, A.M., Rockswold, G., Shi, J., and Panter, S. (2012). Efficacy of reductive ventricular osmotherapy in a swine model of traumatic brain injury. Neurosurgery 70, 445–454.
37. Alam, H.B., Bowyer, M.W., Koustova, E., Gushchin, V., Anderson, D., Stanton, K., Kreishman, P., Cryer, C.M., Hancock, T., and Rhee, P. (2002). Learning and memory is preserved after induced asanguineous hyperkalemic hypothermic arrest in a swine model of traumatic exsanguination. Surgery 132, 278–288.
38. Gao, X., Deng-Bryant, Y., Cho, W., Carrico, K.M., Hall, E.D., and Chen, J. (2008). Selective death of newborn neurons in hippocampal dentate gyrus following moderate experimental traumatic brain injury. J. Neurosci. Res. 86, 2258–2270.
39. Lowenstein, D.H., Thomas, M.J., Smith, D.H., and McIntosh, T.K. (1992). Selective vulnerability of dentate hilar neurons following traumatic brain injury: a potential mechanistic link between head trauma and disorders of the hippocampus. J. Neurosci. 12, 4846–4853.
40. Johnson, V.E., Stewart, J.E., Begbie, F.D., Trojanowski, J.Q., Smith, D.H., and Stewart, W. (2013). Inflammation and white matter degeneration persist for years after a single traumatic brain injury. Brain 136, 28–42.
41. Chiarugi, A. and Moskowitz, M.A. (2003). Poly(ADP-ribose) polymerase-1 activity promotes NF-kappaB-driven transcription and microglial activation: implication for neurodegenerative disorders. J. Neurochem. 85, 306–317.
42. Xu, J., Wang, H., Won, S.J., Basu, J., Kapfhamer, D.. and Swanson, R.A. (2016). Microglial activation induced by the alarmin S100B is regulated by poly(ADP-ribose) polymerase-1. Glia 64, 1869–1878.
43. Vuong, B., Hogan-Cann, A.D., Alano, C.C., Stevenson, M., Chan, W.Y., Anderson, C.M., Swanson, R.A.. and Kauppinen, T.M. (2015). NF-kappaB transcriptional activation by TNF alpha requires phospholipase C, extracellular signal-regulated kinase 2 and poly(ADP-ribose) polymerase-1. J. Neuroinflammation 12, 229.
44. d'Avila, J.C., Lam, T.I., Bingham, D., Shi, J., Won, S.J., Kauppinen, T.M., Massa, S., Liu, J., and Swanson, R.A. (2012). Microglial activation induced by brain trauma is suppressed by post-injury treatment with a PARP inhibitor. J. Neuroinflammation 9, 31.
45. Kauppinen, T.M., Suh, S.W., Berman, A.E., Hamby, A.M., and Swanson, R.A. (2009). Inhibition of poly(ADP-ribose) polymerase suppresses inflammation and promotes recovery after ischemic injury. J. Cereb. Blood Flow Metab. 29, 820–829.
46. Stoica, B.A., Loane, D.J., Zhao, Z., Kabadi, S.V., Hanscom, M., Byrnes, K.R., and Faden, A.I. (2014). PARP-1 inhibition attenuates neuronal loss, microglia activation and neurological deficits after traumatic brain injury. J. Neurotrauma 31, 758–772.
47. Turtzo, L.C., Lescher, J., Janes, L., Dean, D.D., Budde, M.D., and Frank, J.A. (2014). Macrophagic and microglial responses after focal traumatic brain injury in the female rat. J. Neuroinflammation 11, 82.
48. Loane, D.J., Kumar, A., Stoica, B.A., Cabatbat, R., and Faden, A.I. (2014). Progressive neurodegeneration after experimental brain trauma: association with chronic microglial activation. J. Neuropathol. Exp. Neurol. 73, 14–29.
49. Chiu, I.M., Morimoto, E.T., Goodarzi, H., Liao, J.T., O'Keeffe, S., Phatnani, H.P., Muratet, M., Carroll, M.C., Levy, S., Tavazoie, S., Myers, R.M., and Maniatis, T. (2013). A neurodegeneration-specific gene-expression signature of acutely isolated microglia from an amyotrophic lateral sclerosis mouse model. Cell Rep. 4, 385–401.
50. Faden, A.I., Wu, J., Stoica, B.A., and Loane, D.J. (2016). Progressive inflammation-mediated neurodegeneration after traumatic brain or spinal cord injury. Br. J. Pharmacol. 173, 681–691.
51. Rodriguez-Paez, A.C., Brunschwig, J.P., and Bramlett, H.M. (2005). Light and electron microscopic assessment of progressive atrophy following moderate traumatic brain injury in the rat. Acta Neuropathol. (Berl) 109, 603–616.
52. Bramlett, H.M. and Dietrich, W.D. (2002). Quantitative structural changes in white and gray matter 1 year following traumatic brain injury in rats. Acta Neuropathol. 103, 607–614.
53. Johnson, V.E., Stewart, W., and Smith, D.H. (2013). Axonal pathology in traumatic brain injury. Exp. Neurol. 246, 35–43.
54. Brochier, C., Jones, J.I., Willis, D.E., and Langley, B. (2015). Poly(ADP-ribose) polymerase 1 is a novel target to promote axonal regeneration. Proc. Natl. Acad. Sci. U. S. A. 112, 15220–15225.
55. Byrne, A.B., McWhirter, R.D., Sekine, Y., Strittmatter, S.M., Miller, D.M., and Hammarlund, M. (2016). Inhibiting poly(ADP-ribosylation) improves axon regeneration. Elife 5.
56. Wang, X., Sekine, Y., Byrne, A.B., Cafferty, W.B., Hammarlund, M., and Strittmatter, S.M. (2016). Inhibition of Poly-ADP-ribosylation fails to increase axonal regeneration or improve functional recovery after adult mammalian CNS injury. eNeuro 3.
57. Diaz-Arrastia, R., Kochanek, P.M., Bergold, P., Kenney, K., Marx, C.E., Grimes, C.J., Loh, L.T., Adam, L.T., Oskvig, D., Curley, K.C., and Salzer, W. (2014). Pharmacotherapy of traumatic brain injury: state of the science and the road forward: report of the Department of Defense Neurotrauma Pharmacology Workgroup. J. Neurotrauma 31, 135–158.
58. Loane, D.J. and Byrnes, K.R. (2010). Role of microglia in neurotrauma. Neurotherapeutics 7, 366–377.
59. Duhaime, A.C. (2006). Large animal models of traumatic injury to the immature brain. Dev. Neurosci. 28, 380–387.
60. Seok, J., Warren, H.S., Cuenca, A.G., Mindrinos, M.N., Baker, H.V., Xu, W., Richards, D.R., McDonald-Smith, G.P., Gao, H., Hennessy, L., Finnerty, C.C., Lopez, C.M., Honari, S., Moore, E.E., Minei, J.P., Cuschieri, J., Bankey, P.E., Johnson, J.L., Sperry, J., Nathens, A.B., Billiar, T.R., West, M.A., Jeschke, M.G., Klein, M.B., Gamelli, R.L., Gibran, N.S., Brownstein, B.H., Miller-Graziano, C., Calvano, S.E., Mason, P.H., Cobb, J.P., Rahme, L.G., Lowry, S.F., Maier, R.V., Moldawer, L.L., Herndon, D.N., Davis, R.W., Xiao, W., Tompkins, R.G., Inflammation and Host Response to Injury, Large Scale Collaborative Research Program. (2013). Genomic responses in mouse models poorly mimic human inflammatory diseases. Proc. Natl. Acad. Sci. U. S. A. 110, 3507–3512.

Address correspondence to:
Raymond A. Swanson, MD
San Francisco Veterans Affairs Medical Center
127 Neurology
4150 Clement Street
San Francisco, CA 94121

E-mail: raymond.swanson@ucsf.edu